Estimation of inner-domain temperatures for a freezing process

CONFERENCE PAPER · OCTOBER 2014

4 AUTHORS, INCLUDING:

Christoph Josef Backi
Norwegian University of Science and Techno…
10 PUBLICATIONS **7** CITATIONS
SEE PROFILE

John Leth
Aalborg University
39 PUBLICATIONS **85** CITATIONS
SEE PROFILE

Jan Tommy Gravdahl
Norwegian University of Science and Techno…
187 PUBLICATIONS **1,118** CITATIONS
SEE PROFILE

Estimation of inner-domain temperatures for a freezing process

Christoph Josef Backi, Jan Dimon Bendtsen, John Leth and Jan Tommy Gravdahl

***Abstract*— In this paper a state observer for a distributed parameter system (DPS) with nonconstant parameter functions is presented. The DPS describes the freezing of foodstuff in vertical plate freezers and is a nonlinear heat equation. The observer is based upon the Extended Kalman Filter, meaning that the nonlinear heat equation has been discretized in the spatial domain before designing the observer. We show that the observer is robust with respect to perturbations of parameter functions and noisy measurement signals and that the inner-domain temperatures can be correctly estimated.**

I. INTRODUCTION

In order to prevent foodstuff from spoiling while transporting over long distances or storing during long periods, freezing has shown itself superior to many other preservation techniques. This especially holds for fish products, as it is a foodstuff that has a quite short shelf life. Extending shelf life by iced storage is temporally limited, whereas other techniques, like salting or drying have impacts on taste and texture. Therefore gentle freezing and thawing techniques that preserve quality (appearance, taste and odour) are of high interest for the fishing industries worldwide in order to obtain a safe and high quality product.

Freezing time denotes the time it takes to freeze the 'worst point' (the point hardest to affect - depending on geometry and freezing method) down to the safe temperature (mostly $-18\ ^{\circ}\mathrm{C}$). In theory it should suffice to remove a 'theoretical' amount of energy which is defined by the difference between initial and desired temperature plus latent heat of fusion. But as the cold front propagates throughout the spatial domain, the removal of this 'theoretical' amount of energy will not lead to a uniform distribution of temperature. In fact the temperature of the 'worst point' will be higher than the desired temperature. Due to the laws of thermodynamics the overall temperature will uniformly converge to the desired temperature (without disturbances acting on the systems, meaning perfect insulation). However, this procedure is not allowed by some authorities, e.g. the 'regulation of deep-frozen foodstuff' (*Forskrift om dypfryste næringsmidler*) of the *Norwegian Ministry of Health and Care Services* states that before being transported to the storage freezer, the goods must be $-18\ ^{\circ}\mathrm{C}$ at the warmest point.

C.J. Backi (corresponding author) and J.T. Gravdahl are with the Department of Engineering Cybernetics, Norwegian University of Science and Technology, 7491 Trondheim, Norway {backi,gravdahl}@itk.ntnu.no

J.D. Bendtsen and J. Leth are with the Department of Electronic Systems, Aalborg University, 9220 Aalborg, Denmark {dimon,jjl}@es.aau.dk

J. Leth is supported by the Southern Danish Growth Forum and the European Regional Development Fund, under the project "Smart & Cool"

Analytical and numerical models for the freezing of foodstuff have been described by a whole range of publications, see for example [8], where an overview is given about different techniques. Analytical methods deliver freezing time predictions and are often based on *Plank's equation*[1], see [15]. In [13] freezing time predictions for rectangular blocks of foodstuff are described, whereas [12] introduces an extension of Plank's equation for simple shapes. Analytical functions to predict freezing and thawing times for regular and irregular shapes are presented in [6] and [7], respectively. Numerical modelling methods have been described in various publications. A finite-difference scheme for freezing foodstuff is introduced in [14], while [5] presents results for freezing and thawing time prediction by numerical methods. These numerical methods mostly rely on temperature predicting models described by partial differential equations.

Due to the fact that freezing time estimation is often done by simplified analytical means and prior-to-freezing-calculations, the freezing time is often 'overestimated'. Since energy-efficiency has become a big topic in the last two decades due to the finiteness of primary energy carriers as well as their impact on the climate, it is important to gain more knowledge of energy-consuming processes, such as freezing processes. In that sense a better estimation of freezing time could help terminate the freezing process even before the above mentioned analytical methods would suggest.

As computational power has grown significantly in the last decades, it makes sense to introduce real time monitoring and estimation of freezing time; that is, to design state-observers which provide estimates of the non-measurable temperature field in the interior of the good's volume. With this knowledge the freezing time can be estimated. Many observer design methods exist; the most well-known of these is undoubtedly the Kalman Filter for discrete-time systems defined by ordinary differential equations. The Kalman-Bucy-Filter (KBF) is the continuous-time version of the Kalman Filter. Both of these designs rely on linearized system equations and added white Gaussian noise to compensate for modeling and measurement errors. Furthermore there exist so called Extended Kalman Filters (EKF), which utilize the same principle as the aforementioned filters, but instead of linearizing around a fixed setpoint, the linearized system matrix gets updated with full state information at each time-step. In addition, nonlinear observer design methods have been developed in the recent years, as for example [1].

[1]Note that in literature both versions of the name, *Plank* and *Planck*, are used; the correct full name is *Rudolf Plank*, however.

Observers for partial differential equations have gotten more and more attention in the scientific community. In general there exist two ways to attack these problems: *Early lumping* and *late lumping*. In the former approach, the spatial domain is discretized prior to the observer design (finite-dimensional), whereas in the latter, the observer is designed for the PDE itself (infinite-dimensional). An example of an *early lumping* design can be found in [10], where the observer is split up into a finite- and an infinite-dimensional part. Examples of *late lumping* approaches are presented in [16], where an infinite-dimensional sampled data Kalman Filter is introduced and in [11], where transformations are used to reduce the system's complexity prior to designing the observer by backstepping methods. For an overview over different types of PDE observers see [9]. All of the above mentioned designs have one thing in common, namely that all rely on system descriptions with constant parameters, such that transformations (e.g. gauge-transformations) can be used to obtain simplified system structures with known properties. As the system we are investigating is defined by state-dependent parameter functions, however, we cannot use the already established methods. This motivates the subsequent investigation.

The paper is structured as follows: In Section II we will introduce the model equations which will be used for the observer design in Section III. Section IV presents simulation results and Section V will end the paper with concluding remarks and comments on the solution. The used parameters can be found in the appendix.

II. MODEL

The model which is the basis for this observer design is a 2-dimensional parabolic partial differential equation (PDE). The 1-dimensional version of this parabolic PDE has been described earlier in [4], where the PDE was subject to an optimal control problem in order to find an optimal boundary input. Further it has been described in [2], where stability in terms of L^2- and H^1-norms has been proven for classes of input and parameter distribution functions.

The model describes the temperature distribution $T = T(t,x,y)$ throughout a block of fish that is frozen inside a vertical plate freezer

$$\begin{aligned}\rho(T)c(T)T_t &= \big(\lambda(T)T_x\big)_x + \big(\lambda(T)T_y\big)_y \\ &= \lambda_T(T)\big(T_x^2+T_y^2\big) + \lambda(T)\big(T_{xx}+T_{yy}\big)\end{aligned} \tag{1}$$

where $\rho(T)$ denotes the density, $c(T)$ indicates the specific heat capacity at constant pressure and $\lambda(T)$ describes the thermal conductivity. Rewritten, (1) becomes

$$T_t = \kappa(T)\big(T_x^2+T_y^2\big) + k(T)\big(T_{xx}+T_{yy}\big) \tag{2}$$

where $\kappa(T) = \frac{\lambda_T(T)}{\rho(T)c(T)}$ and $k(T) = \frac{\lambda(T)}{\rho(T)c(T)}$.

In order to be well–posed, boundary and initial conditions have to be defined for distributed parameter systems. For the present case it is practical to either choose Dirichlet or Neumann boundary conditions, representing temperature or heat flow at/through the boundary, respectively. Initial conditions represent the initial state of the system. Here it is convenient to choose them evenly distributed throughout the whole spatial domain.

The effects of the freezing medium (vaporizing liquid ammonia) at $x = 0$ and $x = \ell$ as well as of exposure to air ($y = 0$) are modeled by Dirichlet boundary conditions, whereas presumed perfect insulation at the bottom of the fish block ($y = h$) is modeled by Neumann boundary conditions.

The system itself is passive, meaning that the boundary inputs at $x = 0$ and $x = \ell$ are not actively controlled. As an introduction to the upcoming subsections we illustrate in Figure 1 how the spatial domain is discretized and furthermore which of the states are measurable (orange) and which are not (blue). In addition Figure 1 shows how the boundary conditions are chosen and the way they act on the system.

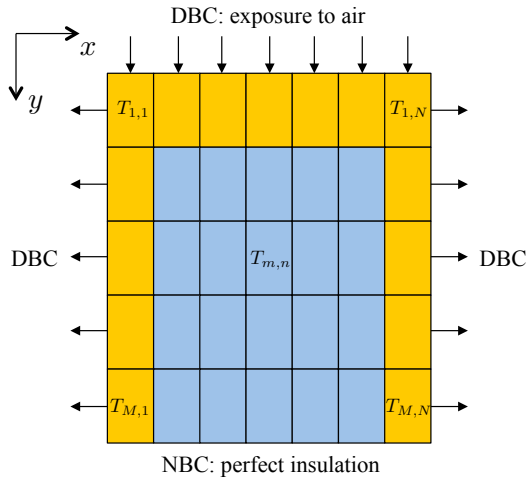

Fig. 1. DBC denotes Dirichlet boundary conditions and NBC denotes Neumann boundary conditions

A. Parameters

The choice of parameter distribution functions $k(T)$ and $\kappa(T)$ has been studied in earlier publications. In [3] the composition of fish tissue as an alloy of different substances is introduced. In [4] and [2] different continuous representations of the parameter functions have been defined, which take the phenomenon of *thermal arrest* caused by *latent heat of fusion* into account. This is achieved by defining a temperature range $\pm\Delta T$ around the freezing point T_F where $c(T)$ is increased significantly in order to slow down heat conduction. The parameter functions in [2] are the basis for this paper and illustrated in Figure 2 for completeness. We remark that $\rho(T)$ is assumed constant over the considered temperature range.

B. Discretization

Discretization is performed by means of finite difference methods for the spatial derivatives only. This corresponds with an *early lumping* approach and will lead to an approximation of the PDE by a set of coupled ODEs. For discretization it is necessary to use uneven discretization

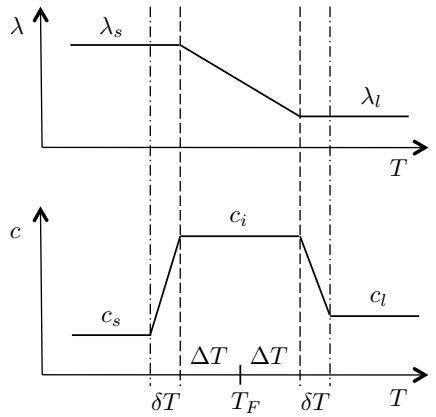

Fig. 2. Parameter function definitions

numbers N and M in x- and y-direction, in order to be able to define central layers for both spatial domains.

The terms T_x and T_y will be approximated by both, first order forward and central difference methods. It is important to mention that, in this case, the discretization direction is not consistent with positive x- and y-directions. This means that discretization is performed from the left/right and from the bottom/top boundaries towards the central layers of the spatial domain using a first order forward difference approach, whereas a first order central difference approach is used at the very center of the spatial domain, both regarding x- and y-directions. The reason for this is that the boundary conditions at $x = 0$ and $x = \ell$ must be imposed to the discretized equations with the same sign (here positive), which will not be the case with a consistent discretization direction.

The following descretizations hold for fixed y- and x-positions, respectively

fixed y-position at m:

$$T_x = \begin{cases} \frac{T_{m,n-1}-T_{m,n}}{\Delta x}, & \text{if } n < \frac{N+1}{2} \\ \frac{T_{m,n+1}-2T_{m,n}+T_{m,n-1}}{2\Delta x}, & \text{if } n = \frac{N+1}{2} \\ \frac{T_{m,n+1}-T_{m,n}}{\Delta x}, & \text{if } n > \frac{N+1}{2}, \end{cases} \tag{3}$$

fixed x-position at n:

$$T_y = \begin{cases} \frac{T_{m-1,n}-T_{m,n}}{\Delta y}, & \text{if } m < \frac{M+1}{2} \\ \frac{T_{m+1,n}-2T_{m,n}+T_{m-1,n}}{2\Delta y}, & \text{if } m = \frac{M+1}{2} \\ \frac{T_{m+1,n}-T_{m,n}}{\Delta y}, & \text{if } m > \frac{M+1}{2}. \end{cases} \tag{4}$$

Note that the terms for $n = \frac{N+1}{2}$ and $m = \frac{M+1}{2}$ in (3) and (4) are obtained by taking half of the 'effect' from both neighbour blocks into account for the block at the center, resulting in a central difference description

$$\frac{T_{m,n+1}-2T_{m,n}+T_{m,n-1}}{2\Delta x} = \frac{1}{2}\frac{T_{m,n-1}-T_{m,n}}{\Delta x} + \frac{1}{2}\frac{T_{m,n+1}-T_{m,n}}{\Delta x}$$

and

$$\frac{T_{m+1,n}-2T_{m,n}+T_{m-1,n}}{2\Delta y} = \frac{1}{2}\frac{T_{m-1,n}-T_{m,n}}{\Delta y} + \frac{1}{2}\frac{T_{m+1,n}-T_{m,n}}{\Delta y}.$$

The approximations for the terms T_{xx} and T_{yy} are obtained by using a second order central difference method. This approach can be applied by following a consistent discretization direction, due to the fact that the boundary conditions enter the discretized equations with the same sign. As a result the following equations hold for fixed y- and x-positions, respectively

fixed y-position at m:

$$T_{xx} = \frac{T_{m,n+1}-2T_{m,n}+T_{m,n-1}}{\Delta x^2}, \tag{5}$$

fixed x-position at n:

$$T_{yy} = \frac{T_{m+1,n}-2T_{m,n}+T_{m-1,n}}{\Delta y^2}. \tag{6}$$

The discrete expressions (3), (4), (5) and (6) are defined for $1 \le n \le N$ and $1 \le m \le M$, where the values at $T_{m,0}$, $T_{m,N+1}$, $T_{0,n}$ and $T_{M+1,n}$ represent the fictional states where the boundary conditions enter the equations. The discretization step sizes are $\Delta x = \frac{\ell}{N}$ and $\Delta x = \frac{h}{M}$.

This discretization procedure will lead to $N \times M$ coupled ordinary differential equations (ODEs). In (7) a general example for how these discretized ODEs look like is demonstrated (for $1 \le n < \frac{N+1}{2}$ and $1 \le m < \frac{M+1}{2}$)

$$\begin{aligned} \dot{T}_{m,n} =& \kappa(T_{m,n})\Big[\Big(\frac{T_{m,n-1}-T_{m,n}}{\Delta x}\Big)^2 + \Big(\frac{T_{m-1,n}-T_{m,n}}{\Delta y}\Big)^2\Big] \\ &+ k(T_{m,n})\Big[\frac{T_{m,n+1}-2T_{m,n}+T_{m,n-1}}{\Delta x^2} \\ &+ \frac{T_{m+1,n}-2T_{m,n}+T_{m-1,n}}{\Delta y^2}\Big]. \end{aligned} \tag{7}$$

C. Boundary conditions

As mentioned before, Dirichlet boundary conditions are imposed on the system at $T_{m,0}$, $T_{m,N+1}$ and $T_{0,n}$. We point out that these boundary conditions are assumed constant and can therefore be defined as $T_{m,0} = T_{m,N+1} = T_{Ammonia}$ for all m (temperature of ammonia) and $T_{0,n} = T_{Air}$ for all n (temperature of air). Furthermore, perfect insulation at the bottom of the fish block is defined by Neumann boundary conditions at $T_{M+1,n}$, leading to the expression $T_{M+1,n} - T_{M,n} = 0$ for all n.

III. OBSERVER

The observer is designed to estimate the unmeasurable states inside the spatial domain of the fish block. Inner-domain measurements are neither practical nor possible for the system setup. The estimation of the unmeasurable states is important to predict when the desired temperature is reached inside the inner layers of the spatial domain. Thus it can replace simpler, approximative freezing time prediction methods, as already mentioned in Section I.

A first choice for a practical observer design is often a Kalman Filter based design. Due to the fact that a Kalman Filter is a well-established observer in engineering practice, it is often used as a benchmark in order to compare other

observer designs with regard to performance. The Kalman Filter has certain robustness properties which are based on the fact that modeling and measurement errors are introduced to the system model by adding up white Gaussian noise signals w and v to the state derivatives and the outputs, respectively. Here we will investigate the possibility of implementing an Extended Kalman Filter (EKF).

A. Design

As can be seen in Fig. 3 the design relies on a nonlinear model running in parallel to the plant. Both, plant and model base on the same spatially discretized equations of the PDE (2) and are fed with the same inputs, namely the boundary conditions at $x = 0$, $x = \ell$ ($T_{Ammonia}$) and $y = 0$ (T_{Air}). The boundary conditions at $y = h$ are directly embedded in the spatially discretized equations of the plant and the model.

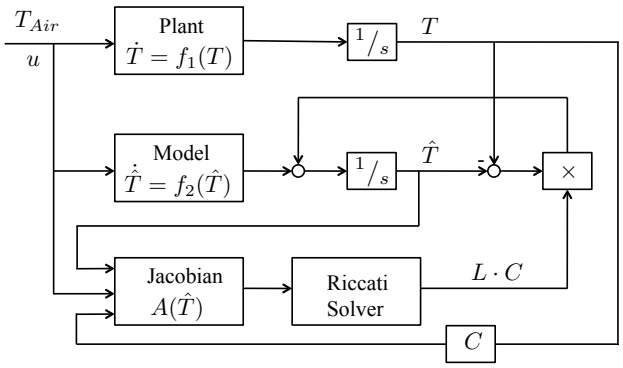

Fig. 3. Design schematic

In contrast to standard designs, the Jacobian $A(\hat{T}) = \frac{\partial f_2}{\partial \hat{T}}$ is only used as an input to the Riccati equation and thus to compute the observer feedback gain L. Note that in order to calculate $A(\hat{T})$, the nonmeasurable states are taken from the model, whereas the measurable states are taken from the plant.

B. Linearization

One of the basic principles of an EKF is that the nonlinear system has to be linearized, but not around a fixed set-point (equilibrium) like the *Kalman-Bucy-Filter*, but around changing setpoints defined by the solutions to the (linearized) ODEs. Thus the system matrix $A(\hat{T})$ represents the linearized system's behavior at particular points in state-space and changes as the system is progressing in time.

We define the state vector as

$$T = \begin{bmatrix} T_{1,1} \cdots T_{1,N} & T_{2,1} \cdots T_{2,N} & \cdots & T_{M,N} \end{bmatrix}^T.$$

By linearizing the discretized version of (2) we obtain a sparse matrix $A(\hat{T})$ with a regular pattern of diagonal and side-diagonal entries. Note that the system matrix can be subject to change due to the definition of the chosen parameter functions and also to the discretization scheme.

C. Measurements

It is assumed that no in-domain measurements are available, thus it is only possible to measure temperatures at the boundaries. This means that the output is

$$y = \begin{bmatrix} T_{1,1} & \cdots & T_{1,N} & T_{2,1} & T_{2,N} & \cdots & T_{M,1} & T_{M,N} \end{bmatrix}^T$$

which results in an output matrix on the following form

$$C = \text{blockdiag}\begin{bmatrix} C_1 & C_2 & \cdots & C_M \end{bmatrix}$$

where $C_1 = I_{(N\times N)}$ and $C_k = \begin{bmatrix} 1 & 0_{(1\times N-1)} \\ 0_{(1\times N-1)} & 1 \end{bmatrix}$ for $2 \leq k \leq M$.

D. Riccati equation

In this setup we use the matrix Riccati differential equation in the form

$$\dot{P} = A(\hat{T})P + PA^T(\hat{T}) - PC^T R^{-1} CP + Q \tag{8a}$$

$$L = PC^T R^{-1} \tag{8b}$$

where R and Q represent the noise-covariance matrices of the signals w and v, respectively. These matrices typically have entries exclusively on the diagonals, as a correlation among states and among outputs are neglected. Furthermore, we assume no correlation between single states and outputs. As P is a function of $A(\hat{T})$, the feedback gain is actually a function of time, $L = L(t)$.

IV. SIMULATION

Simulations have been conducted for a non-standard case, where white Gaussian noise was added to the measurements in order to investigate how the observer handles this phenomenon. The white noise was normed by its largest value, such that values between ± 1 K were added to the measurements. This corresponds (to some degree) with the specifications of measurement equipment, such as e.g. thermocouples[2]. Furthermore, to illustrate robustness, the parameters of the observer differ from those of the plant. In fact we chose the area of thermal arrest to be double the size for the observer, $\Delta T_{EKF} = 2\Delta T_{Sys}$, and the observers' parameter functions are 2 times larger than those of the system, meaning $k_{EKF} = 2k_{Sys}$ and $\kappa_{EKF} = 2\kappa_{Sys}$.

Simulation parameters can be found in the Appendix. The observer parameters were tuned by simulations and the initial conditions of the plant and the observer differ by 3 K. The values for N and M present a trade-off between accuracy and performance, as spatial resolution is limited by computational power. In addition, temperature variations along the y-coordinates for fixed x-positions are small, but not negligible. This justifies to choose M quite small, but bigger than 1 ($M = 1$ represents a 1-dimensional PDE). Figure 4 shows plots for different x-coordinates at a fixed y-position (top layer of the fish block). The boundary layer can be seen in the top left, followed by the top right, bottom left and bottom right as we move along the x-axis towards

[2]The standard EN 60584 defines three accuracy classes, where the first allows deviations of maximal ± 1.5 K.

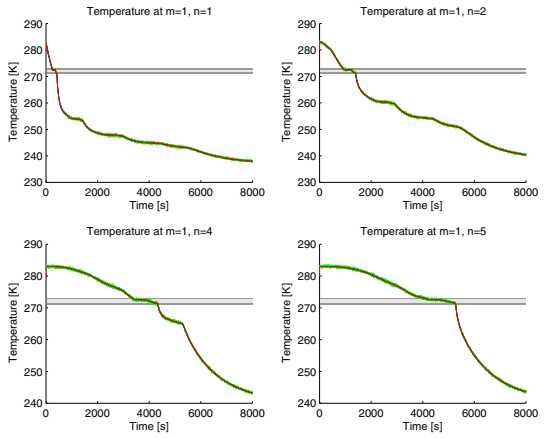

Fig. 4. Observer states (red), real states (blue) and noisy measurement signals (green) at $m = 1$ and $n = 1, 2, 4, 5$

the center of the domain. The center is shown in the plot in the bottom right. The area of thermal arrest is illustrated by the two gray areas (dark corresponds with ΔT_{EKF}, light with ΔT_{Sys}). The observer states are displayed in red, whereas the plant's states are shown in blue. The noisy measurement signal is illustrated in green.

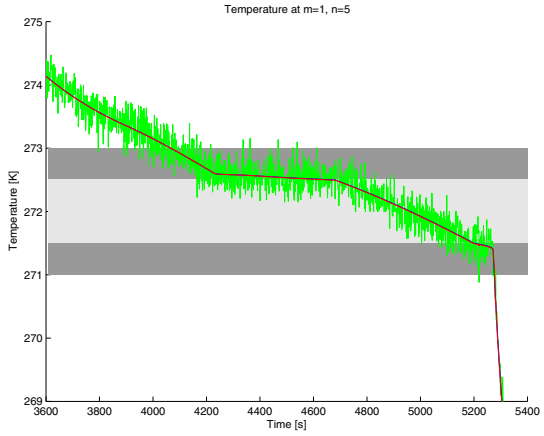

Fig. 5. Zoom of observer state (red), real state (blue) and noisy measurement signal (green) at $m = 1$ and $n = 5$

In Figure 5 a zoom into the bottom right plot in Figure 4 is illustrated. Due to the fact that the state can be measured, the observer state is following the real state quite accurately, even in the presence of white Gaussian noise.

Figure 6 presents plots for different x-coordinates at the center of the y-coordinate ($m = 3$). Only the top left plot includes the noisy measurement signal, as it is the only measurable state in the set of illustrated states. As can be seen the observer follows the real states quite satisfying.

Figure 7 shows a zoom into the bottom right plot in Figure 6. Comparing this to Figure 5, one can see that now in the absence of measurement, the observer doesn't follow the real state as accurately.

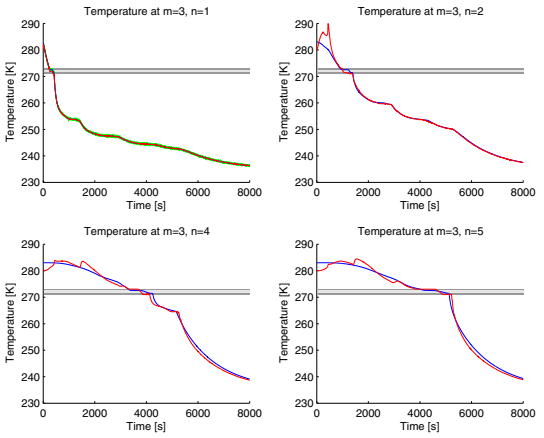

Fig. 6. Observer states (red), real states (blue) and noisy measurement signals (green) at $m = 3$ and $n = 1, 2, 4, 5$

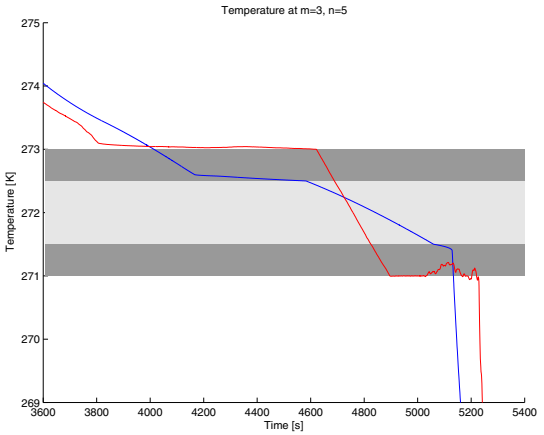

Fig. 7. Zoom of observer state (red) and real state (blue) at $m = 3$ and $n = 5$

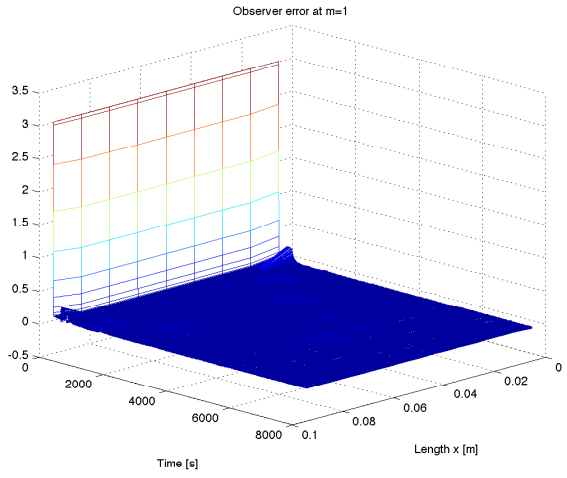

Fig. 8. Observer error at $m = 1$

In Figures 8 and 9 the error between real and observed state is shown along the x-coordinate for a fixed y-position

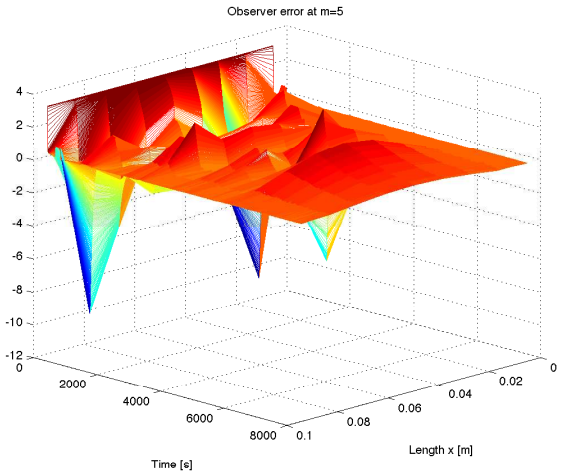

Fig. 9. Observer error at $m = 5$

(top and bottom of the block, respectively). It can be seen that the error is brought back to zero for both cases, even in the presence of noisy measurements and diverging parameters.

V. CONCLUSION

In this paper we presented an observer design for a distributed parameter system (DPS) describing the freezing of foodstuff, in particular fish, in vertical plate freezers. The DPS is a partial differential equation (PDE) in the form of a nonlinear heat equation. The observer is based upon an Extended Kalman Filter (EKF) with the purpose of estimating the temperature distribution inside the inner spatial domain of the fish block.

The results presented in Section IV show that the non-measurable states in the inner domain get estimated quite accurately, even in the case of differing parameter functions chosen for the observer and the plant, respectively. Furthermore the presence of white Gaussian noise in the measurement signals is handled well by the observer. Thus it can be concluded that the design is robust to parameter variations and noise.

REFERENCES

[1] M. Arcak and P. Kokotovic. Nonlinear observers: a circle criterion design and robustness analysis. *Automatica*, 37:1923–1930, 2001.

[2] C.J. Backi, J.D. Bendtsen, J. Leth, and J.T. Gravdahl. The nonlinear heat equation with state–dependent parameters and its connection to the burgers' and the potential burgers' equation. In *Proceedings of the 19th IFAC World Congress*, Cape Town, South Africa, 2014.

[3] C.J. Backi and J.T. Gravdahl. Modeling of the freezing process for fish in vertical plate freezers. In *Proceedings of the 17th Nordic Process Control Workshop*, Copenhagen, Denmark, 2012.

[4] C.J. Backi and J.T. Gravdahl. Optimal boundary control for the heat equation with application to freezing with phase change. In *Proceedings of the 3rd Australian Control Conference*, Perth, Australia, 2013.

[5] D.J. Cleland, A.C. Cleland, and R.L. Earle. Prediction of freezing and thawing times for multi-dimensional shapes by numerical methods. *International Journal of Refrigeration*, 10:32–39, 1987.

[6] D.J. Cleland, A.C. Cleland, and R.L. Earle. Prediction of freezing and thawing times for multi-dimensional shapes by simple formulae part 1: regular shapes. *International Journal of Refrigeration*, 10:156–164, 1987.

[7] D.J. Cleland, A.C. Cleland, and R.L. Earle. Prediction of freezing and thawing times for multi-dimensional shapes by simple formulae part 2: irregular shapes. *International Journal of Refrigeration*, 10:234–240, 1987.

[8] A.E. Delgado and D.-W. Sun. Heat and mass transfer models for predicting freezing processes – a review. *Journal of Food Engineering*, 47:157–174, 2001.

[9] Z. Hidayat, R. Babuska, B. De Schutter, and A Nunez. Observers for linear distributed-parameter systems: A review. In *Proceedings of the 2011 IEEE International Symposium on Robotic and Sensors Environment (ROSE)*, Montreal, Canada, 2011.

[10] T. Kobayashi and S. Hitotsuya. Observers and parameter determination fir distributed parameter systems. *International Journal of Control*, 33(1):31–50, 1981.

[11] M. Krstic and A. Smyshlyaev. *Boundary Control of PDEs - A Course on Backstepping*. Advances in Design and Control. Society for Industrial and Applied Mathematics, 2008.

[12] Q.T. Pham. Extension to planck's equation for predicting freezing times of foodstuffs of simple shapes. *International Journal of Refrigeration*, 7(6):377–383, 1984.

[13] Q.T. Pham. Analytical method for predicting freezing times of rectangular blocks of foodstuffs. *International Journal of Refrigeration*, 8(1):43–47, 1985.

[14] Q.T. Pham. A fast, unconditionally stable finite-difference scheme for heat conduction with phase change. *International Journal of Heat and Mass Transfer*, 28:2079–2085, 1985.

[15] R. Plank. Beiträge zur Berechnung und Bewertung der Gefriergeschwindigkeit von Lebensmitteln. *Zeitschrift für die gesamte Kälte-Industrie*, (10), 1941.

[16] S.A. Sallberg, P.S. Maybeck, and M.E. Oxley. Infinite-dimensional sampled-data kalman filtering and the stochastic heat equation. In *Proceedings of the 49th IEEE Conference on Decision and Control*, Atlanta, GA, USA, 2010.

APPENDIX

ℓ	0.1	m
h	0.5	m
N	9	[-]
M	5	[-]
T_F	272	K
$T_{init,EKF}$	280	K
$T_{init,Sys}$	283	K
ΔT_{EKF}	1	K
ΔT_{Sys}	0.5	K
δT	0.1	K
$T_{Ammonia}$	235	K
T_{Air}	278	K
c_s	2200	$\mathrm{Jkg^{-1}K^{-1}}$
c_l	3800	$\mathrm{Jkg^{-1}K^{-1}}$
c_i	283000	$\mathrm{Jkg^{-1}K^{-1}}$
ρ	950	$\mathrm{kgm^{-3}}$
λ_s	1.8	$\mathrm{Wm^{-1}K^{-1}}$
λ_l	0.5	$\mathrm{Wm^{-1}K^{-1}}$

$$C = \begin{bmatrix} \Gamma & 0 & 0 & 0 & 0 \\ 0 & \Psi & 0 & 0 & 0 \\ 0 & 0 & \Psi & 0 & 0 \\ 0 & 0 & 0 & \Psi & 0 \\ 0 & 0 & 0 & 0 & \Psi \end{bmatrix}$$

$$R = 10 \begin{bmatrix} \Gamma & 0 & 0 & 0 & 0 \\ 0 & \Sigma & 0 & 0 & 0 \\ 0 & 0 & \Sigma & 0 & 0 \\ 0 & 0 & 0 & \Sigma & 0 \\ 0 & 0 & 0 & 0 & \Sigma \end{bmatrix}$$

$$Q = 10 \begin{bmatrix} \Gamma & 0 & 0 & 0 & 0 \\ 0 & \Phi & 0 & 0 & 0 \\ 0 & 0 & \Phi & 0 & 0 \\ 0 & 0 & 0 & \Phi & 0 \\ 0 & 0 & 0 & 0 & \Phi \end{bmatrix}$$

with $\Gamma = I_{(9\times 9)}$, $\Psi = \begin{bmatrix} 1 & 0_{(1\times 8)} \\ 0_{(1\times 8)} & 1 \end{bmatrix}$, $\Sigma = \begin{bmatrix} 10 & 0 \\ 0 & 10 \end{bmatrix}$ and $\Phi = \mathrm{diag}(\begin{bmatrix} 1 & 10 & 10 & 10 & 1 & 10 & 10 & 10 & 10 \end{bmatrix})$.